Quantum-information-processing architecture with endohedral fullerenes in a carbon nanotube

W. L. Yang,[1] Z. Y. Xu,[1,2] H. Wei,[3] M. Feng,[1,*] and D. Suter[4,†]

[1]*State Key Laboratory of Magnetic Resonance and Atomic and Molecular Physics, Wuhan Institute of Physics and Mathematics, Chinese Academy of Sciences, Wuhan 430071, People's Republic of China*

[2]*Graduate School of the Chinese Academy of Sciences, Beijing 100049, People's Republic of China*

[3]*Center for Modern Physics and Department of Physics, Chongqing University, Chongqing 400044, People's Republic of China*

[4]*Fakultät Physik, Technische Universität Dortmund, D-44221 Dortmund, Germany*

(Received 6 December 2009; published 5 March 2010)

A potential quantum-information processor is proposed using an array of the endohedral fullerenes $^{15}N@C_{60}$ or $^{31}P@C_{60}$ contained in a single walled carbon nanotube (SWCNT). The qubits are encoded in the nuclear spins of the doped atoms, while the electronic spins are used for initialization and readout, as well as for two-qubit operations.

DOI: 10.1103/PhysRevA.81.032303 PACS number(s): 03.67.Lx, 03.65.Ud, 73.21.−b

I. INTRODUCTION

Quantum-information processing (QIP) has attracted considerable attention over the last years, since it allows one to efficiently solve computational problems that have no efficient solution in classical computer science [1,2]. Unleashing this potential requires the design of quantum-information processors that control a large number of qubits. Among the interesting qubit candidates are endohedral fullerenes $^{15}N@C_{60}$ or $^{31}P@C_{60}$ [3–8] whose decoherence times are longer than those of most other candidates. Quantum gate operations on these qubits can be implemented by electron spin resonance (ESR) and nuclear magnetic resonance (NMR) techniques.

The endohedral atoms (^{15}N or ^{31}P) have electron spins as well as nuclear spin degrees of freedom. The electron spins are particularly well suited for individual addressing, for coupling neighboring qubits, and for readout. The nuclear spins, in contrast, are not coupled to each other, and their decoherence time is particularly long. It appears therefore useful to combine these properties and use the nuclear as well as the electronic spin for quantum-information processing [4–8]. This combination can also solve some problems associated with the fact that the electronic spin is not a two-level system, but has $S = 3/2$.

One of the main obstacles for implementing such fullerene-based quantum computers is the lack, until now, of a single-qubit readout capability [9,10]. Here, we would like to discuss a system that might solve this difficulty. We consider a row of endohedral fullerenes $^{15}N@C_{60}$ or $^{31}P@C_{60}$ enclosed in a single walled carbon nanotube (SWCNT). This system has been called fullerene peapod. Such systems have been studied experimentally [11,12]. One of the attractive features of the SWCNT is that it allows transport of mobile electrons [12], which could be used to read out the state of the electron spins in the peapod. This idea is sketched in Fig. 1 where the doped fullerenes are positioned as a line in a SWCNT. Using the mobile electrons on the SWCNT may help to solve the problem of the single-spin readout, which was left open in earlier proposals [4–8].

Our article is structured as follows. In Sec. II we present our system architecture and work through the requirements for implementing universal quantum computation [13]. This includes one-qubit and two-qubit gating, initialization, and readout. Sec. III discusses some details that arise when large quantum registers are implemented. Sec. IV gives the requirements that must be met by such an apparatus and discusses some issues related to its realization. The article ends with a short summary in Sec. V.

II. THE MODEL

A. System and Hamiltonian

The system that we consider consists of a linear chain of endohedral fullerenes confined in a SWCNT, as sketched in Fig. 1. The ^{31}P nuclear spins represent the qubits, while the electronic spins provide ancilla qubits for coupling the nuclear spin qubits to each other. Between gate operations, the electron spin state does not contain quantum information and we are free to choose the state most suitable to our purpose. In the following, we will assume that it is in the $m_s = +3/2$ state.

We label the states of the auxiliary qubits $|3/2\rangle_S = |\uparrow\rangle_S$ and $|-3/2\rangle_S = |\downarrow\rangle_S$. The states of the nuclear spins encoding the qubits are $|1/2\rangle_I = |\uparrow\rangle_I$ and $|-1/2\rangle_I = |\downarrow\rangle_I$. The system is placed in a magnetic field oriented along the peapod axis. The i^{th} qubit experiences a field,

$$\vec{B}_i = \left[B_0 + \frac{dB}{dz} z_i\right] \vec{e}_z,$$

where dB/dz is the magnetic field gradient, $\vec{e}_z$ is a unit vector along the axis of the peapod, z_i is the position of the i^{th} qubit from the origin, and B_0 is the strength of the magnetic field at the origin.

The electronic spins of neighboring molecules interact by dipole-dipole couplings. As in relevant articles published previously, we only take the nearest-neighbor interactions into account and find for the system Hamiltonian,

$$H = \sum_{i=1}^{N} \left\{\Omega_S^i S_z^i - \Omega_I^i I_z^i + A S_z^i I_z^i\right\} + \sum_{i=1}^{N-1} D_{i,i+1} S_z^i S_z^{i+1}, \quad (1)$$

where the first two terms are the electronic and nuclear Zeeman splitting, the third term denotes the hyperfine interaction, and

*mangfeng@wipm.ac.cn
†dieter.suter@uni-dortmund.de

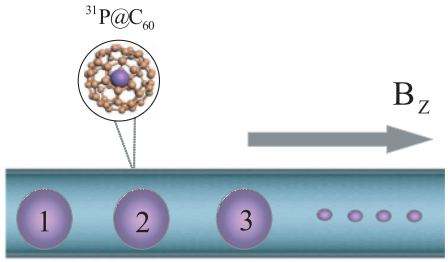

FIG. 1. (Color online) Schematic setup of ^{31}P@C$_{60}$@SWCNT system, where the fullerene molecules ^{31}P@C$_{60}$ are trapped equidistantly. A magnetic field gradient, generated by micropatterned wires, is applied.

the last term represents the secular part of the magnetic dipolar interaction between the nearest-neighbor electronic spins. The electron spin Larmor frequency is $\Omega_S^i = g\mu_B B_i$, the nuclear spin Larmor frequency $\Omega_I^i = \gamma_I B_i$, μ_B is the Bohr magneton, g is the Land é g factor of the electron, γ_I is the gyromagnetic ratio of the nucleus, A the hyperfine coupling strength, and $D_{i,i+1}$ is the nearest-neighbor dipole-dipole coupling strength. We have omitted the couplings between nuclear spins because they are too small and use frequency units, where $\hbar = 1$. We have truncated the dipolar coupling operator with respect to the difference of the electron spin Larmor frequencies. The validity of this approximation depends on the magnetic field gradient and on the distance between the qubits. For a nearest-neighbor distance of $r = 2.91$ nm and a magnetic field gradient of 4×10^5 T/m, the relevant resonance frequencies of the electron spin $|3/2\rangle_S \leftrightarrow |-3/2\rangle_S$ transitions differ by 97.2 MHz, while the coupling strength is of the order of 3 MHz. Under these conditions, the truncation is therefore an excellent approximation.

B. Quantum gate operations for a single fullerene

Consider a single C$_{60}$ molecule in a SWCNT under an external magnetic field B_0. The Hamiltonian of Eq. (1) reduces then to

$$H_1 = \Omega_S^0 S_z - \Omega_I^0 I_z + A S_z I_z, \tag{2}$$

where $\Omega_S^0 = g\mu_B B_0$ and $\Omega_I^0 = \gamma_I B_0$. For ^{31}P and ^{15}N, the hyperfine interaction strength $A/2\pi$ are about 138.4 MHz and 21.2 MHz, respectively [3]. For most of the specific data in the article, we will use the number from ^{31}P, but the concept is equally applicable to both molecules. In a field of $B_0 = 1$ T, the Larmor frequencies of the electron and the ^{31}P nuclear spins are $\Omega_S^0/2\pi \approx 28$ GHz and $\Omega_I^0/2\pi \approx 17.2$ MHz, respectively. Straightforward calculations yield the energies of the eigenstates as listed in Table I.

Figure 2 represents the energies of the spin states and identifies them by the spin states. Figure 3 shows the magnetic dipole transitions between these states, which correspond to a change of the nuclear spin quantum number by one unit (left-hand side, NMR) or the electron spin (right-hand side, ESR). The electron spin transitions have the frequencies $\Omega_S^0 \pm A/2$ and fall therefore into the microwave frequency range (≈ 28 GHz in a field of 1 T). The nuclear spin transition frequencies are $3A/2 \pm \Omega_I^0$ and $A/2 \pm \Omega_I^0$ and fall into the radiofrequency (RF) range (≈70–210 MHz).

TABLE I. Energies of the spin Hamiltonian Eq. (2).

Nuclear spin	Electron spin	Energy
$\|1/2\rangle_I$	$\|3/2\rangle_S$	$3\Omega_S^0/2 + \Omega_I^0/2 - 3A/4$
$\|1/2\rangle_I$	$\|1/2\rangle_S$	$\Omega_S^0/2 + \Omega_I^0/2 - A/4$
$\|1/2\rangle_I$	$\|-1/2\rangle_S$	$-\Omega_S^0/2 + \Omega_I^0/2 + A/4$
$\|1/2\rangle_I$	$\|-3/2\rangle_S$	$-3\Omega_S^0/2 + \Omega_I^0/2 + 3A/4$
$\|-1/2\rangle_I$	$\|3/2\rangle_S$	$3\Omega_S^0/2 - \Omega_I^0/2 + 3A/4$
$\|-1/2\rangle_I$	$\|1/2\rangle_S$	$\Omega_S^0/2 - \Omega_I^0/2 + A/4$
$\|-1/2\rangle_I$	$\|-1/2\rangle_S$	$-\Omega_S^0/2 - \Omega_I^0/2 - A/4$
$\|-1/2\rangle_I$	$\|-3/2\rangle_S$	$-3\Omega_S^0/2 - \Omega_I^0/2 - 3A/4$

Resonant microwave pulses are well suited for generating quantum gate operations in spin qubits. However, if we apply them to the $S = 3/2$ electron spin, they usually mix the (ancilla-) qubit states $|\pm 3/2\rangle_S$ with the unused $|\pm 1/2\rangle_S$ states, thus causing loss of quantum information. This is not the case for π rotations around an axis in the xy plane, so we only use this type of operation on the electron spins. Specifically, the flip of the electronic spin by the inversion operation,

$$\hat{P} = e^{-i\pi S_x} = i \begin{pmatrix} 0 & 0 & 0 & 1 \\ 0 & 0 & 1 & 0 \\ 0 & 1 & 0 & 0 \\ 1 & 0 & 0 & 0 \end{pmatrix},$$

exchanges the states $|+1/2\rangle_S \leftrightarrow |-1/2\rangle_S$ and $|+3/2\rangle_S \leftrightarrow |-3/2\rangle_S$ but does not mix the subspaces spanned by $|\pm 3/2\rangle_S$ and by $|\pm 1/2\rangle_S$. If the $\hat{P}$ operation is generated by a frequency-selective pulse tuned to the appropriate component of the hyperfine doublet, we obtain a CNOT$_{IS}$ operation, as required in the sequences described below.

In the following, we will need to SWAP information between the electron and nuclear spin. In terms of spin states, this corresponds to

$$|3/2\rangle_S |-1/2\rangle_I \leftrightarrow |-3/2\rangle_S |1/2\rangle_I ,$$

which cannot be induced by a single RF or microwave pulse. It can, however, be decomposed into CNOT operations,

$$\begin{aligned} \text{SWAP}_{SI} &= \text{CNOT}_{SI} \cdot \text{CNOT}_{IS} \cdot \text{CNOT}_{SI}, \\ &= \text{CNOT}_{IS} \cdot \text{CNOT}_{SI} \cdot \text{CNOT}_{IS}, \end{aligned} \tag{3}$$

where CNOT$_{SI}$ (CNOT$_{IS}$) is the controlled-NOT operation acting on the nuclear (electron) spin, controlled by the electron

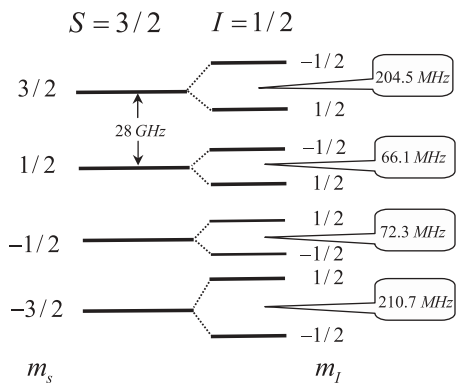

FIG. 2. Energies of a single endohedral fullerene ^{31}P@C$_{60}$.

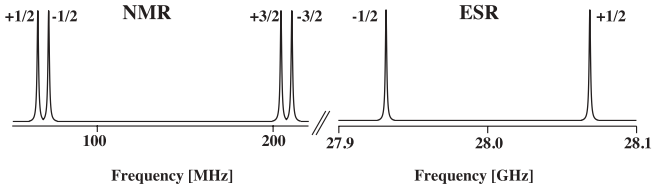

FIG. 3. Magnetic-dipole transitions for a single endohedral fullerene $^{31}P@C_{60}$. The left-hand spectrum corresponds to the nuclear spin transitions (NMR), the right-hand part to the electron spin transitions (ESR). Each transition of the nuclear spin is labeled with the corresponding m_S value of the electron spin and the electron spin transitions are labeled with the nuclear spin states.

(nuclear) spin. The first decomposition corresponds to the exchange of the states,

$$\begin{aligned} |3/2\rangle_S|-1/2\rangle_I &\leftrightarrow |3/2\rangle_S|1/2\rangle_I \\ |-3/2\rangle_S|1/2\rangle_I &\leftrightarrow |3/2\rangle_S|1/2\rangle_I \\ |3/2\rangle_S|-1/2\rangle_I &\leftrightarrow |3/2\rangle_S|1/2\rangle_I . \end{aligned} \tag{4}$$

Each of these CNOT gates can be implemented by a selective microwave or RF pulse; the CNOT_{SI}, for example, corresponds to a π rotation of the nuclear spin, conditional on the electron spin being in the $m_S = +3/2$ state. As can be seen from Figs. 2 and 3, this can be implemented as a $\hat{P}$ operation by an RF pulse with the frequency of 204.5 MHz (in a field of 1 T).

We are now left with the task of implementing arbitrary single-qubit operations on the nuclear spin qubit. This can in principle be accomplished with the help of resonant RF pulses, as in NMR quantum computing [14,15]. However, these pulses would have to compete with the hyperfine coupling. Direct application of an RF field that is strong enough to make the effect of the hyperfine coupling negligible would not only be technically very challenging, it would also strongly violate the rotating wave approximation and thereby lead to a very poor fidelity of the gate operation. Instead, it will be much easier and result in higher fidelity, if the single-qubit operations are implemented by pairs of RF pulses applied simultaneously at the frequencies 204.5 MHz and 210.7 MHz. One of these RF fields will implement the operation conditional on the electron spin being in the logical 0 state, the other if the electron spin is in the logical 1 state. The combined effect thus corresponds to an unconditional gate operation.

C. Extended quantum registers

Large and therefore powerful quantum registers can be implemented by extended chains of qubits. The different qubits can be addressed in frequency space by applying a magnetic field gradient. For the Hamiltonian of Eq. (1), the transition frequencies of every electron spin split into 16 transitions, whose frequencies depend on the state of the neighboring electron spin, and which are up to fourfold degenerate, as shown in Fig. 4 and Table II.

As discussed in Sec. II B, single-qubit operations can be implemented directly on the nuclear spin. Since the nuclear spin transitions are the same for qubits in extended chains as for isolated qubits, all the nuclear spin operations remain the same. We do, however, have to modify the electron

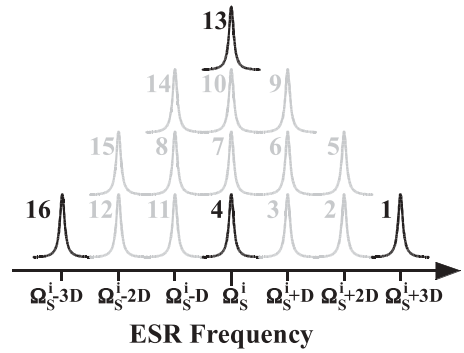

FIG. 4. Schematic representation of the transition frequencies of the electron spins in a linear chain of fullerene qubits. The central transition frequency Ω_S^i corresponds to the frequency of an isolated electron spin and includes contributions from the magnetic field gradient and the nuclear hyperfine interaction. D is the coupling constant. Transitions between states that are not populated in an ideal quantum processor are gray.

spin operations, for example, the selective inversion of the electron spin discussed in the second line of Eq. (4). The single resonance line that has to be inverted in the case of an isolated qubit corresponds now to 16 lines at seven frequencies. Single-qubit gate operations applied to qubit i have to excite all these transitions equally, since they must not depend on the states of the neighboring qubits. This is a rather challenging task, which can be implemented by multifrequency excitation [16]. The task can be simplified if we assume that our quantum-information processor works under ideal conditions: in this case, only the $\pm 3/2$ states are occupied, and we can disregard all transitions in which one of the neighboring qubits is in the states $\pm 1/2$. These transitions are grayed in Fig. 4 and in normal typeface in Table II. This leaves us with four transitions at frequencies Ω_S^i, $\Omega_S^i \pm 3D$, as shown in bold in Table II and as black lines in Fig. 4.

TABLE II. List of the transition frequencies of the electronic spin versus the corresponding states of the neighboring electron spins. Transitions that occur in an ideal quantum-information processor are in boldface.

No.	State of neighbor qubits	Transition frequency
1	$\mathbf{\lvert 3/2, 3/2\rangle}$	$\mathbf{\Omega_S^i + 3D}$
2	$\lvert 3/2, 1/2\rangle$	$\Omega_S^i + 2D$
3	$\lvert 3/2, -1/2\rangle$	$\Omega_S^i + D$
4	$\mathbf{\lvert 3/2, -3/2\rangle}$	$\mathbf{\Omega_S^i}$
5	$\lvert 1/2, 3/2\rangle$	$\Omega_S^i + 2D$
6	$\lvert 1/2, 1/2\rangle$	$\Omega_S^i + D$
7	$\lvert 1/2, -1/2\rangle$	$\mathbf{\Omega_S^i}$
8	$\lvert 1/2, -3/2\rangle$	$\Omega_S^i - D$
9	$\lvert -1/2, 3/2\rangle$	$\Omega_S^i + D$
10	$\lvert -1/2, 1/2\rangle$	Ω_S^i
11	$\lvert -1/2, -1/2\rangle$	$\Omega_S^i - D$
12	$\lvert -1/2, -3/2\rangle$	$\Omega_S^i - 2D$
13	$\mathbf{\lvert -3/2, 3/2\rangle}$	$\mathbf{\Omega_S^i}$
14	$\lvert -3/2, 1/2\rangle$	$\Omega_S^i - D$
15	$\lvert -3/2, -1/2\rangle$	$\Omega_S^i - 2D$
16	$\mathbf{\lvert -3/2, -3/2\rangle}$	$\mathbf{\Omega_S^i - 3D}$

D. Two-qubit gates

We now consider two-qubit operations between neighboring qubits $(i-1, i)$ in an extended chain of fullerene molecules. All such operations start with SWAP_{SI} operations on the molecules participating in the two-qubit operation. The central part of our two-qubit gate consists of the CNOT_{i-1i} gate or the controlled phase flip CPF_{i-1i} acting on a nearest-neighbor pair of electron spins. The gate ends with a second pair of SWAP_{SI} operations on the molecules participating in the two-qubit operation. The net effect of this sequence of operations is that the two nuclear spins have undergone the CNOT_{i-1i} (or CPF_{i-1i}) operation, while the electron spins return to their initial state (which we assume to be the $m = +3/2$ ground state). This assures that the passive electron spins are always in the $m = +3/2$ state, as we assumed in the preceding subsection. Furthermore, it minimizes the effect of decoherence, since this is the thermal equilibrium state at low temperature and therefore not affected by relaxation.

Considering now the central part of the two-qubit operation, the $\mathrm{CNOT}_{i-1,i}$ gate between the electron spins, inspection of Table II shows that it can be implemented by applying π pulses to transitions 1 and 4; this implements an operation NOT on qubit i conditional on the qubit $i-1$ being in state $+3/2$ and unconditional with respect to the state of qubit $i+1$. Unfortunately, a π pulse applied to transition 4 will also invert transition 13, which is degenerate with transition 4, and which corresponds to qubit $i-1$ being in state $-3/2$ and therefore invalidates the CNOT operation. This difficulty can be eliminated by various approaches, including multifrequency excitation of several transitions. Alternatively, we may take into account that qubit $i+1$ is not active during a $\mathrm{CNOT}_{i-1,i}$ operation, that is, the information is in the nuclear spin, and the state of the electron spin is the state into which it was initialized (i.e., the $|+3/2\rangle_S$ state). This eliminates the need to invert transition 4 and makes the π pulse on transition 1 a perfect $\mathrm{CNOT}_{i-1,i}$ operation.

In an extended quantum register, we also have to consider that the operations on the nuclear spins will affect all nuclei in the quantum register (i.e., also passive qubits, which should not be affected by the specific gate operations). If we try to make the pulses on the nuclear spins sufficiently weak, so that their effect on the passive qubits is negligible, they will become unacceptably slow: with the parameters as discussed above, the difference in the Larmor frequencies of neighboring nuclear spins is only on the order of 10 Hz (for ^{31}P). It will then be advantageous to use hard pulses that simultaneously affect all nuclear spins. Since the only operations applied to the nuclear spins in our scheme are the SWAP_{SI} operations of Eq. (3), this turns out not to be a problem: For the passive qubits, where the CNOT_{IS} operations are identity operations, the first version of the SWAP_{SI} gate becomes $\mathrm{CNOT}_{SI}\ \mathrm{CNOT}_{SI} = 1$, while the second version becomes CNOT_{SI}. Since all operations (one- and two-qubit) involve pairs of SWAP_{SI} gates, even the second version leaves passive qubits invariant.

E. Initialization and readout

The proposed system can be initialized into the ground state by relaxation of the electron spins: In a field of $B = 1$T, at a temperature $T = 0.1$ K, the equilibrium ground-state

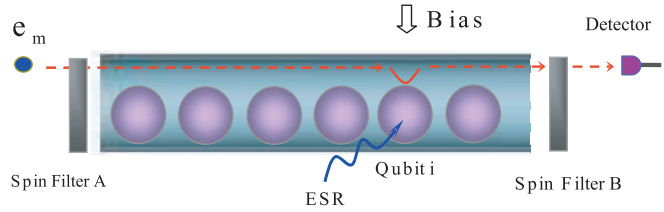

FIG. 5. (Color online) Scheme for the detection of the state of electron spins inside a fullerene embedded in a SWCNT. The spin filter $A(B)$ located in the front (back) of the SWCNT only allows the down(up)-polarized electrons to pass. The bias stops the mobile electron along the SWCNT at a place above the caged spin and an ESR pulse generates a CNOT operation between the mobile and the caged electron spins.

population is > 0.99999. This electron spin polarization can be transferred to the nuclear spin qubits by a SWAP operation.

Readout may be accomplished by using mobile electrons on the outside of the peapod. Various schemes have been developed for the detection of single spins [17–20], which cannot be applied directly to the spins of electrons in C_{60} cages. Nevertheless, this can also be achieved, by coupling the caged spin to external spins and converting the spin degree of freedom to charges, then detecting the charges [9,10].

This can also be achieved in the present system, as shown schematically in Fig. 5. The electrons used for detection are spin polarized by passing them through a spin filter and guiding them along the SWCNT by applying suitable bias fields. At the position of the qubit that is to be read out, the mobile electron is stopped by adjusting the bias field. The separation between the mobile and the caged electrons is small enough that a sizable magnetic dipole-dipole coupling exists between them. We may then write the Hamiltonian of the two electron spins as

$$H_{\mathrm{sub}} = \Omega_S^i S_z^i + \Omega_S^m S_z^m + D' S_z^i S_z^m, \tag{5}$$

where S_z^i is the spin operator of the caged qubit electron $(S = 3/2)$ and S_z^m the spin of the mobile electron $(S = 1/2)$, and D' represents the strength of the coupling between the mobile and the caged spins. For a separation of 0.8 nm, the dipole coupling strength would be of the order of 100 MHz. Depending on the state of the caged electron $(m = \pm 3/2)$, the transition frequency of the mobile electron is thus shifted from its Larmor frequency Ω_S^m by $\pm 3/2D'$.

This can be used for a detection mechanism: If we want to detect the $m = +3/2$ state of the caged electron, we send a stream of electrons along the SWCNT, which are spin polarized in the spin filter A. This spin filter can be made from ferromagnetic materials [21], or semiconductor quantum dots [22]. When the electrons are trapped near qubit i, we apply a microwave pulse with frequency $\Omega_S^m + 3/2D'$ and a flip angle of $\approx \pi$. This operation corresponds to a CNOT operation conditional on the caged spin being in the $m = +3/2$ state and thus to a COPY operation. The mobile spin is then transported further down along the SWCNT and through spin filter B, which is oriented such that it only allows those electrons to pass whose spin has been flipped. This procedure can be repeated as often as necessary to get a sufficient signal at the

detector. Here, we have only considered the coupling between the mobile electron and the nearest qubit. The couplings to the other qubits are at least 30 times smaller. The additional small line splittings and line broadenings arising from these long-range couplings do not significantly affect the precision of the readout mechanism.

III. BEYOND THE NEAREST-NEIGHBOR APPROXIMATION

A. Non-nearest-neighbor couplings

So far, we have considered only interactions between nearest neighbors. In reality, dipolar interactions exist between any pair of spins. In a linear chain, the strength $D_{i,k}$ of the interaction between qubits i and k decreases as

$$D_{i,k} \propto \left(\frac{1}{|i-k|}\right)^3. \tag{6}$$

Figure 6 illustrates the effect of the non-nearest neighbor couplings. The uppermost spectrum corresponds to the case of nearest neighbors only (i.e., to the situation discussed in Sec. II). If we add non-nearest neighbors [trace (b)], each resonance line splits into seven lines separated by $D_{\rm nn}/8$, where $D_{\rm nn}$ is the coupling between nearest neighbors. The weight of the lines (1:2:3:4:3:2:1) is given by the number of states of the next-nearest neighbors; the outermost lines correspond to the next-nearest neighbors being in the $|+3/2,+3/2\rangle$ or both in the $|-3/2,-3/2\rangle$ state. The lines with relative amplitude 2 correspond to the coupling partners being in the $|+3/2,+1/2\rangle$ or $|+1/2,+3/2\rangle$ state for one line or $|-3/2,-1/2\rangle$ or $|-1/2,-3/2\rangle$ for the other line.

Adding a third pair of qubits causes an additional splitting of each line into a (1:2:3:4:3:2:1) multiplet, with line separation $D_{\rm nn}/64$. With the resolution of the figure [see trace (c)], this appears as a line broadening. Clearly, this is an undesirable situation, which would cause significant decoherence. This situation can be corrected if we take into account the fact that all electron spins of the passive qubits are in the $\uparrow$ ($m_S = +3/2$) state, since the quantum information was SWAPed into the nuclear spin. This situation is depicted in trace (d), where all but the nearest-neighbor qubits are taken to be in the $\uparrow$ state. As a result, we do not obtain a splitting of the resonance line, but a shift by $-3D_{\rm nn}/7 \approx -0.429 D_{\rm nn}$.

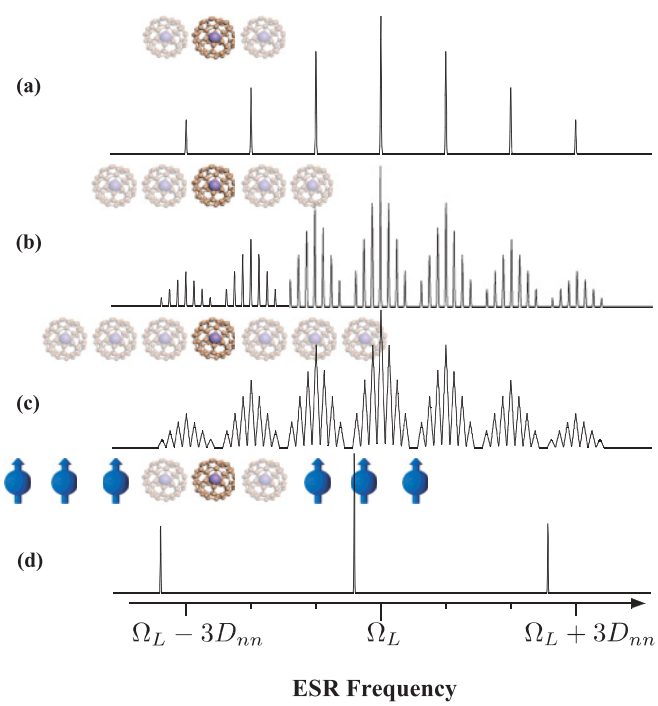

FIG. 6. (Color online) Transitions of a single qubit in the presence of couplings to other qubits as a function of the chain length. (a) Nearest neighbors only. (b) Nearest neighbors and next-nearest neighbors. (c) Three qubits on each side. (d) Infinite chain, where all but the nearest neighbors are polarized. Ω_L is the Larmor frequency of the central qubit and $D_{\rm nn}$ is the nearest-neighbor coupling strength.

B. Quantum state transfer

Universal quantum computation requires two-qubit operations between all qubit pairs. If the pair is not directly coupled by dipolar interaction, this usually requires a series of SWAP operations between nearest neighbors. Our present schemes allows us to avoid this overhead by using a mobile electron. As for the readout, we assume that this mobile electron travels in the conduction band of the semiconducting carbon nanotube hosting the fullerenes. Its motion is controlled by external bias electrodes.

We consider an array of identical ^{31}P@C$_{60}$ placed in a SWCNT as shown in Fig. 7. As described in Sec. II E, it is possible to exchange a quantum state between the stationary qubit and the mobile electron spin. We may therefore use the mobile electron spin as a bus qubit. If we want to transfer quantum information between the stationary qubits i and k, we first move the electron to qubit i and perform a SWAP operation, using the appropriate ESR pulse sequence. We then move the mobile electron to position k, perform a second SWAP operation, and move it back to position i for a third SWAP operation. This completes the SWAP$_{ik}$ operation.

The caged spin is well protected from external perturbations, but decoherence experienced by the mobile electron spin may be faster. Nevertheless, decoherence times of the order of 10 μs have been reported [23], which would make it comparable to the relaxation times of the N@C$_{60}$ in the peapods [24] and be long enough to perform SWAP operations

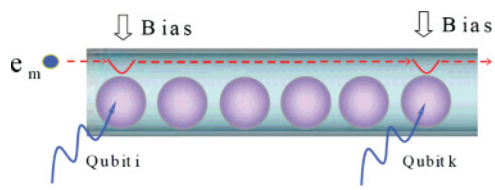

FIG. 7. (Color online) Scheme for transferring a quantum state between two qubits i and k using the spin of the mobile electron as a bus qubit. The bias voltages localize the electron at the appropriate positions; the ESR pulses (shown as wavy arrows) induce SWAP operations between the stationary and the bus qubit.

as well as fast transport of the mobile electron compared to the decoherence time.

IV. FEASIBILITY

The preceding sections presented a design for a scalable quantum computer. For this concept to become reality, a number of engineering challenges have to be overcome. Here, we discuss the design parameters that have to be reached to make such a device useful.

A. Addressing qubits

Addressing the individual electronic spins requires that they are distinguishable in frequency space. This is achieved by applying a magnetic field gradient, which shifts the individual electron spin resonance. One difficulty with the frequency-space addressing is that we must avoid generating overlap between the hyperfine-split resonances of the individual qubits. Furthermore, we have assumed that we work in the weak-coupling limit, where the frequency differences between adjacent qubits are large compared to the dipole-dipole coupling constant. Although this is not a necessary requirement [25], it simplifies the design of quantum gate operations.

If we choose the separation between adjacent qubit molecules as $\Delta z = 2.9$ nm, we obtain a dipole-dipole coupling constant of the order of 3 MHz. If we wish to stay in the weak-coupling limit, the separation between the Larmor frequencies of neighboring electron spins should then be at least 30 MHz. As shown in Fig. 8(a), this allows no more than three to four molecules in a row before the resonance frequencies of the higher-frequency lines of the hyperfine doublet start to overlap with the frequency range of the lower-frequency lines of some other molecules. As shown in Fig. 8(b), it is nevertheless possible to add more molecules without generating overlap, provided the frequency separation between the qubits is chosen correctly. An alternative approach is depicted in Fig. 8(c): Here, we assume that the difference between the Larmor frequencies of adjacent molecules is large compared to the hyperfine splitting, thus avoiding any spectral overlap between neighboring molecules. This choice of parameters may be most suitable for $^{15}N@C_{60}$ molecules, where the hyperfine splitting is significantly smaller than for $^{31}P@C_{60}$.

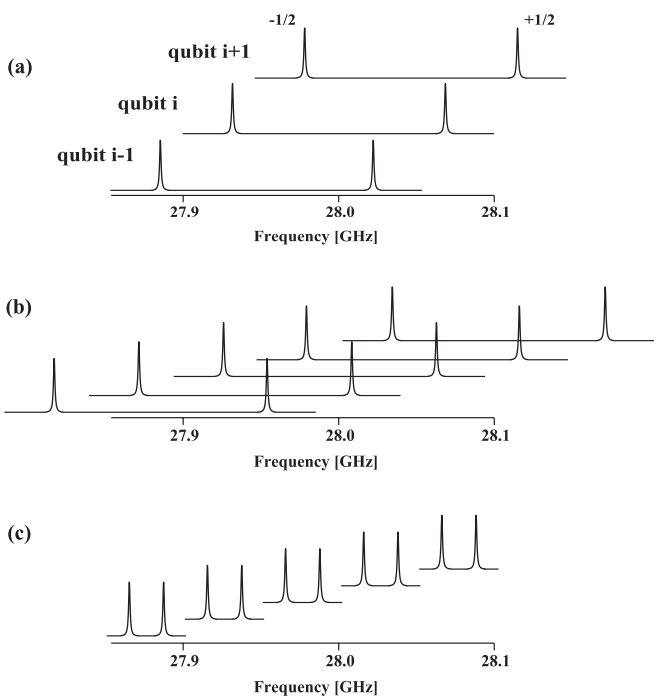

FIG. 8. Schemes for addressing electron spin qubits in a magnetic field gradient. (a) Three $^{31}P@C_{60}$ molecules, separated by $\Delta\Omega = 2\pi \times 45$ MHz. (b) Five $^{31}P@C_{60}$ molecules, separated by $\Delta\Omega = 2\pi \times 55$ MHz. (c) Five $^{15}N@C_{60}$ molecules, separated by $\Delta\Omega = 2\pi \times 55$ MHz.

Compared to the electron spin resonance frequencies, the nuclear Larmor frequencies are smaller by 3–4 orders of magnitude. In the field gradient considered here, this would correspond to frequency differences of the order of only 5 kHz for ^{15}N and 20 kHz for ^{31}P for the parameters used above. Selective addressing of the nuclear spins thus requires that the duration of the selective RF pulses should be at least several hundred μs, which may be undesirable for fast gate operations. A good solution could be the use of hard (short) RF pulses that excite all nuclear spins. As described in the previous sections, each SWAP operation between the electron and nuclear spins includes an even number of π pulses acting on the nuclear spins. For the nuclear spins of the passive qubits, the SWAP operations result in a NOP, as required.

B. Experimental challenges

Although the quantum architecture discussed here appears attractive and physically feasible, its implementation faces several formidable challenges. Several proposals have been put forward for injecting and moving polarized electrons on SWCNT [26–28]. Turning those into useful devices for quantum computing will require precise control by electrodes that allow one to move the mobile electrons between the required positions without affecting the quantum mechanical superposition states of their spin degrees of freedom. Currently, there are no data available about the relevant decoherence times for the spins of these mobile electrons. The closest references are from electrons in SWCNT-based single-electron devices [12]. Since the relevant decoherence mechanism is not yet fully understood, it is difficult to extrapolate. Depending on the mechanism and parameters, it may be possible to use dynamic decoupling techniques [29,30] to reduce the decoherence.

In the main part of the article, we have considered exchange of information between different parts of the quantum register by direct dipolar interactions or with the help of a mobile electron spin acting as a bus qubit. If these approaches prove too difficult to scale to many-qubit quantum registers, it might be worth considering a distributed quantum computer based on many small peapod quantum registers. They could be connected via the Bell-state analyzer discussed in Ref. [31], which is designed to entangle two electron spins. As shown in Ref. [32], passing the mobile electrons from different C_{60}@SWCNTs through the Bell-state analyzers could entangle the caged electron spins in

different C_{60}@SWCNTs, as required for building a quantum network [33]. To build the Bell-state analyzers, however, we have to develop beam splitters for the electrons and suitable charge detectors. Although there has been some progress in these aspects [34,35], these devices are not yet available [35].

Additional challenges are associated with the peapod itself: Depending on the system parameters, the distances between the molecules may vary, and the molecules may be arranged in zig-zag form rather than in a straight line [28]. In natural abundance, the 1% fraction of carbon nuclei that carry a nuclear spin (^{13}C) will contribute to the decoherence in the system. Clearly, this effect can be reduced by using isotopically pure material, as has been demonstrated, for example, in diamond [36]. Clearly, these challenges are difficult but may be overcome eventually. It will be interesting to watch progress in this area.

V. CONCLUSION

In summary, we have proposed a scheme for performing universal quantum computation in a C_{60}@SWCNT (peapod) system. We have discussed how to efficiently implement the quantum logical gate operations required for universal quantum computation. Transfer of information between qubits was considered by direct dipole-dipole couplings or by using a mobile electron spin as a bus qubit. Although our scheme cannot be realized with today's technology, it appears possible that the currently existing obstacles can be overcome as nanotechnology makes further progress.

ACKNOWLEDGMENTS

This work is supported by the National Natural Science Foundation of China under Grant No. 10774163 and by the Robert Bosch Stiftung.

[1] P. W. Shor, SIAM J. Comput. **26**, 1484 (1997).
[2] L. K. Grover, Phys. Rev. Lett. **79**, 325 (1997).
[3] W. Harneit, C. Meyer, A. Weidinger, D. Suter, and J. Twamley, Phys. Status Solidi (b) **233**, 453 (2002); J. J. L. Morton, A. M. Tyryshkin, A. Ardavan, S. Benjamin, K. Porfyrakis, S. A. Lyon, and G. A. D. Briggs, *ibid.* **243**, 3028 (2006).
[4] W. Harneit, Phys. Rev. A **65**, 032322 (2002).
[5] D. Suter and K. Lim, Phys. Rev. A **65**, 052309 (2002).
[6] J. Twamley, Phys. Rev. A **67**, 052318 (2003).
[7] M. Feng and J. Twamley, Phys. Rev. A **70**, 032318 (2004).
[8] C. Ju, Dieter Suter, and J. Du, Phys. Rev. A **75**, 012318 (2007).
[9] M. Feng and J. Twamley, Phys. Rev. A **70**, 030303(R) (2004).
[10] M. Feng and J. Twamley, Europhys. Lett. **69**, 699 (2005); J. Twamley, D. W. Utami, H-S Goan, and G. Milburn, New J. Phys. **8**, 63 (2006); M. Feng, G. J. Dong, and B. Hu, *ibid.* **8**, 252 (2006).
[11] B. W. Smith, M. Monthioux, and D. E. Luzzi, Nature (London) **396**, 323 (1998).
[12] P. Utko, J. Nygard, M. Monthioux, and L. Noe, Appl. Phys. Lett. **89**, 233118 (2006); B. Gao, D. C. Glattli, B. Placais, and A. Bachtold, Phys. Rev. B **74**, 085410 (2006); C. H. L. Quay, J. Cumings, S. J. Gamble, A. Yazdani, H. Kataura, and D. Goldhaber-Gordon, *ibid.* **76**, 073404 (2007).
[13] D. P. DiVincenzo, Fortschr. Phys. **48**, 771 (2000).
[14] D. Suter and T. S. Mahesh, J. Chem. Phys. **128**, 052206 (2008).
[15] L. M. K. Vandersypen and I. L. Chuang, Rev. Mod. Phys. **76**, 1037 (2005).
[16] P. P. Borbat, R. H. Crepeau, and J. H. Freed, J. Magn. Reson. **127**, 155 (1997).
[17] D. Rugar, C. S. Yannoni, and J. A. Sidles, Nature (London) **360**, 563 (1992); G. P. Berman, G. D. Doolen, P. C. Hammel, and V. I. Tsifrinovich, Phys. Rev. Lett. **86**, 2894 (2001); Phys. Rev. B **61**, 14694 (2000).
[18] Y. Manassen, I. Mukhopadhyay, and N. R. Rao, Phys. Rev. B **61**, 16223 (2000).
[19] W. Wernsdorfer and R. Sessoli, Science **284**, 133 (1999); A. Caneschi, D. Gatteschi, C. Sangregorio, R. Sessoli, L. Sorace, A. Cornia, MA. Novak, C. Paulsen, and W. Wernsdorfer, J. Magn. Magn. Mater. **200**, 182 (1999); C. I. Pakes, P. W. Josephs-Franks, R. P. Reed, S. G. Corner, and M. S. Colclough, IEEE Trans. Instrum. Meas. **50**, 310 (2001).
[20] H. Park, J. Park, A. K. L. Lim, E. H. Anderson, A. P. Allvisatos, and P. L. McEuen, Nature (London) **407**, 57 (2000).
[21] J. S. Moodera, R. Meservey, and X. Hao, Phys. Rev. Lett. **70**, 853 (1993).
[22] H.-A. Engel and D. Loss, Phys. Rev. Lett. **86**, 4648 (2001); P. Recher, E. V. Sukhorukov, and D. Loss, *ibid.* **85**, 1962 (2000).
[23] C. Galland and A. Imamoglu, Phys. Rev. Lett. **101**, 157404 (2008).
[24] S. Tóth, D. Quintavalle, B. Náfrádi, L. Korecz, L. Forró, and F. Simon, Phys. Rev. B **77**, 214409 (2008).
[25] T. S. Mahesh and Dieter Suter, Phys. Rev. A **74**, 062312 (2006).
[26] L. P. Kouwenhoven, A. T. Johnson, N. C. van der Vaart, C. J. P. M. Harmans, and C. T. Foxon, Phys. Rev. Lett. **67**, 1626 (1991). This turnstile injector was based on a GaAs quantum dot, but it might also be applicable to a semiconducting SWCNT [27, 28], which has a similar band structure.
[27] D. Gunlycke, J. H. Jefferson, T. Rejec, A. Ramsak, D. G. Pettifor, and G. A. D. Briggs, J. Phys. Condens. Matter **18**, S851 (2006).
[28] S. C. Benjamin, A. Ardavan, G. A. D. Briggs, D. A. Britz, D. Gunlycke, J. Jefferson, M. A. G. Jones, D. F. Leigh, B. W. Lovett, A. N. Khlobystov, S. A. Lyon, J. J. L. Morton, K. Porfyrakis, M. R. Sambrook, and A. M. Tyryshkin, J. Phys. Condens. Matter **18**, S867 (2006).
[29] L. Viola and S. Lloyd, Phys. Rev. A **58**, 2733 (1998).
[30] J. J. L. Morton, A. M. Tyryshkin, A. Ardavan, S. C. Benjamin, K. Porfyrakis, S. A. Lyon, and G. A. D. Briggs, Nat. Phys. **2**, 40 (2006).
[31] C. W. J. Beenakker, D. P. DiVincenzo, C. Emary, and M. Kindermann, Phys. Rev. Lett. **93**, 020501 (2004); X. L. Zhang, M. Feng, and K. L. Gao, Phys. Rev. A **73**, 014301 (2006).
[32] W. L. Yang, H. Wei, X. L. Zhang, and M. Feng, Phys. Rev. A **78**, 054301 (2008).

[33] H. J. Kimble, Nature (London) **453**, 1023 (2008).

[34] M. Henny, S. Oberholzer, C. Strunk, T. Heinzel, K. Ensslin, M. Holland, and C. Schönenberger, Science **284**, 296 (1999); W. D. Oliver, J. Kim, R. C. Liu, and Y. Yamamoto, *ibid.* **284**, 299 (1999); E. Buks, R. Schuster, M. Heiblum, D. Mahalu, and V. Umansky, Nature (London) **391**, 871 (1998).

[35] J. M. Elzerman, R. Hanson, L. H. Willems van Beveren, B. Witkamp, L. M. K. Vandersypen, and L. P. Kouwenhoven, Appl. Phys. Lett. **84**, 4617 (2004).

[36] G. Balasubramanian, P. Neumann, D. Twitchen, M. Markham, R. Kolesov, N. Mizuochi, J. Isoya, J. Achard, J. Beck, J. Tissler, V. Jacques, P. R. Hemmer, F. Jelezko, and J. Wrachtrup, Nat. Mater. **8**, 383 (2009).